PHYSICAL REVIEW B VOLUME 31, NUMBER 8 15 APRIL 1985

Fluctuating dipoles and polarizabilities in ionic materials: Calculations on LiF

P. W. Fowler
University Chemical Laboratory, Lensfield Road, Cambridge CB2 1EW, England

P. A. Madden
Physical Chemistry Laboratory, South Parks Road, Oxford OX1 3QZ, England
(Received 23 July 1984)

The physical mechanisms responsible for the fluctuating polarization which causes light scattering and infrared absorption in ionic materials are investigated by electronic structure calculations on distorted crystal lattices. The lattice is modeled at two levels which permit the separation of the effects of electrostatic and first-shell overlap interactions. The distortion-induced polarization may be regarded as the sum of an asymptotic term, which includes the electrostatically induced moments described by a multipole expansion, and the result of a change in shape of the confining potential well in which an ion sits. The latter is significant only for short-range distortions. The confining well is caused by both electrostatic and overlap interactions, and for first-shell distortions the two act in concert. Both the asymptotic and confining potential effects may be built into a computationally tractable model for the fluctuating polarization of crystalline LiF; extended schemes for more disordered situations, such as the melt, are considered.

I. INTRODUCTION

The light-scattering spectrum of a condensed ionic material in the Rayleigh wing region (1—500 cm^{-1}) contains information on the relative motion of ions which may be difficult to obtain by other means. For example, Mazzacurati *et al.*[1,2] have shown that very large changes in the polarization characteristics of this spectrum accompany an order-disorder transition of the Ag^+ ions in AgI in the superionic conduction regime. Recently, an extensive study of the Rayleigh wing spectra of molten alkali halides has been undertaken[3] in order to observe the charge density wave expected in a two-component charged fluid.

The corresponding "interaction-induced" spectra in nonionic, weakly interacting ("van der Waals") fluids such as argon[4] or CS_2 (Ref. 5) are now understood at a quantitative level,[6] the understanding has developed through three stages. The electrodynamic mechanisms responsible for the interaction-induced polarizability, whose fluctuations are observed in the spectra, may be identified and studied in the gas phase,[7] where small numbers of molecules interact. The applicability of the same mechanisms to the condensed-phase polarizability may be examined by comparing the results of computer simulations with experiment.[8,9] With the dependence of the fluctuating polarizability upon the coordinates of the molecules identified, it is then possible to reexpress the polarizability in terms of whatever modes are convenient for a theoretical description of the intermolecular motion in the condensed material, and in this way account for the shape of the spectroscopic line.[6]

This sequence cannot be followed in ionic materials, and a theory of Rayleigh wing spectra for them has not been developed. The reason is that the first stage cannot be replicated, the electrodynamic interactions between small numbers of ions in the gas phase are a poor guide to the condensed-phase behavior.[10] In order to relate the fluctuating polarizability to the intermolecular coordinates in a condensed ionic material it is necessary to study the condensed phase itself.

In the present paper we will examine, by electronic structure calculations, the dipoles (and quadrupoles) in distorted crystal lattices of LiF in the presence and absence of external fields. The idea behind this work is that the weakly distorted lattice can provide a good model system in which the essential many-body aspects of the electrodynamics of condensed ionic systems are present, yet which is sufficiently simple, by virtue of symmetry, for us to extract the information we require. The distorted lattice is, in this sense, the analog of the low-density gas in the study of van der Waals materials. Our objective is to provide closed expressions for the dependence of the interaction-induced properties on the ionic coordinates. Our calculations are made on only weakly distorted lattices, and so the application of these expressions to strongly disordered materials, such as melts, may be questioned. However, the expressions will be designed so that they give correctly the effect of one ion on another when the distance between the two is large. It is for such configurations that the crystal and melt differ most, as computer simulations show.[11] Consequently, we expect that our expressions should provide a reasonable approximation to the fluctuating property in the condensed phase; clearly this viewpoint should be tested by computer simulation, as in the analogous second stage of the procedure used to explain the spectra of condensed van der Waals materials. Although our introductory remarks (and much of the subsequent discussion) focus on the light-scattering problem, we will also present results on the interaction-induced di-

poles and quadrupoles. The latter are primarily of interpretative interest, but the induced dipoles are responsible for the far infrared spectra.

II. GENERAL BACKGROUND

The theoretical description of the dielectric properties of a material whose electrons may be considered localized on the constituent molecules is well established. Within the dipole approximation[12] the instantaneous polarization, $\vec{P}(\vec{r})$, is given by

$$\vec{P}(\vec{r})=\sum_i \vec{p}^{\,i}\delta(\vec{r}-\vec{r}^{\,i}) , \tag{1}$$

where $\vec{p}^{\,i}$ and $\vec{r}^{\,i}$ are the total dipole moment and position of molecule i. $\vec{p}^{\,i}$ is given by

$$\vec{p}^{\,i}=\vec{\mu}^{\,i}+\overleftrightarrow{\alpha}^{i}\cdot\left[\vec{E}^{\,0}(\vec{r}^{\,i})+\sum_{j\,(\neq i)}\overleftrightarrow{T}(\vec{r}^{\,ij})\cdot\vec{p}^{\,i}\right] , \tag{2}$$

where $\vec{E}^{\,0}$ is the field produced by external charges, $\overleftrightarrow{T}(\vec{r})$ is the dipole-dipole tensor $(\vec{\nabla}\vec{\nabla}r^{-1})$, and $\vec{\mu}^{\,i}$ and $\vec{\alpha}^{\,i}$ are the instantaneous values of the dipole moment and dipole polarizability of molecule i. In general, $\vec{\mu}^{\,i}$ and $\overleftrightarrow{\alpha}^{i}$ *depend upon the configuration of all N molecules in the sample.*

For nonpolar materials, Eqs. (1) and (2) lead to the Clausius-Mossotti or Lorenz-Lorentz equation for the permittivity,[13]

$$\frac{\epsilon-1}{\epsilon+2}=(4\pi\rho/3)\langle\overleftrightarrow{\alpha}^{1}\rangle , \tag{3a}$$

where ρ is the density. This equation is accurately obeyed by the fluids and crystals of nonpolar, van der Waals compounds with $\langle\overleftrightarrow{\alpha}^{1}\rangle$ simply taken to be the mean value of the gas-phase, isolated molecule polarizability.[14] That is, so far as the equilibrium property ϵ of such materials is concerned, Eqs. (1) and (2) with the $\vec{R}^{\,N}$ dependence of $\overleftrightarrow{\alpha}^{i}$ neglected appear to give a good description of the electrodynamic interactions between the molecules.

The application of these equations, and the underlying localized electron assumption, to the dielectric properties of condensed ionic materials is much less firmly established. The static permittivities of ionic crystals have been analyzed by the Clausius-Mossotti equation, e.g., for simple MX salts,[15]

$$\frac{\epsilon-1}{\epsilon+2}=(4\pi\rho/3)(\alpha_{M^+}+\alpha_{X^-}) , \tag{3b}$$

where α_{M^+} and α_{X^-} are *in-crystal* polarizabilities of the cation and anion. For some ionic compounds, notably the alkali halides,[15,16] the in-crystal polarizabilities are reasonably transferable from one material to another. The in-crystal anion polarizability is much smaller than the value calculated for the free ion, whereas for the cation the two values are usually quite similar.[17] In other cases, that of materials containing the O^{2-} ion is well documented,[15,16] the application of Eq. (4) to the data requires that $\alpha_{O^{2-}}$ depends strongly on the counterion. From these observations one may conclude that, at best, the localized electron assumption may hold in ionic materials but that, in any case, the ionic polarizabilities depend strongly on the positions of the other ions in the medium.

In a number of recent papers we have investigated the validity of the concept of an in-crystal ionic polarizability by *ab initio* electronic structure calculations[10,18,19] on clusters of ions in environments appropriate to crystal lattices. Our calculated values for alkali and halide ions agree closely with those deduced from the application of Eq. (3) to experimental data and have been shown to be insensitive to charge-transfer effects in the crystal.[10,18,20] The observed variation of the in-crystal polarizability of O^{2-} may be accounted for by the effects of the different local environments of the ion in different materials, *within* the localized electron model.[19]

In a perfect cubic crystal the electrostatic potential felt by an electron due to neighboring ions may be written

$$V(r)=V_0(r)+V_4(r)P_4(\hat{r}_z)+V_6(r)P_6(\hat{r}_z)+\cdots , \tag{4}$$

where P_l is an lth-order Legendre polynomial. The effects of the crystalline environment of the polarizability of a first or second row ion is dominated by the spherical (V_0) term. For such ions the ground-state wave function is well represented by an sp basis, these functions are unaffected by the V_4 and higher-order terms in the potential. To describe the first-order perturbed wave function in a uniform, externally applied field (which determines the polarizability), additional functions of d type are required. As is well known, the V_4 potential splits a set of d functions about a mean value determined by the V_0 potential. We have shown that this effect on the first-order wave function does not affect the polarizability [98% of the effect of the crystalline environment on the polarizability of F^- is due to V_0 (Ref. 19)]. The V_4 part of the potential only becomes significant when d orbitals are occupied in the unperturbed ion [as, for example, in the case of Ag^+ (Ref. 20)]. For anions the spherical part of the electrostatic potential may be viewed as a spherical potential well which tends to compress the electron cloud. It is illustrated in Figs. 1 and 2 where we show, for later refer-

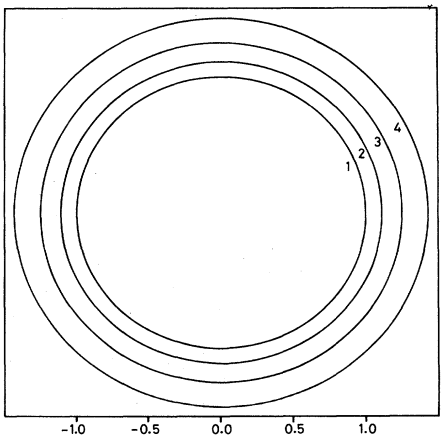

FIG. 1. Spherically averaged potential energy of an electron in an octahedron of (+1) charges. The six charges are disposed on a sphere of radius R and the figure is a slice through the equatorial plane $-3/2R \leq x,y \leq 3/2R$. Contours (counting out from the center) at 1ϵ, 0.9ϵ, 0.8ϵ, and 0.7ϵ, where ϵ is the well depth $-6/R$.

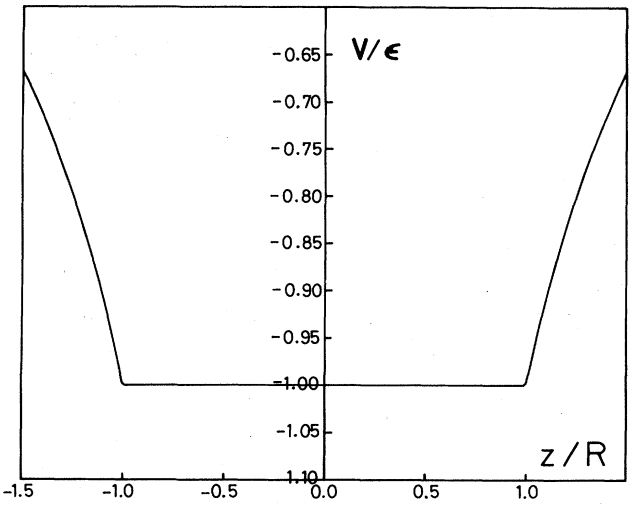

FIG. 2. Spherically averaged potential energy of an electron in an octahedron of (+ 1) charges. The graph is a section along the z axis of the potential described in Fig. 1. V is in units of ϵ and z in units of R.

ence, a contour plot and simple graph of $V_0(r)$ for an octahedral shell of charges. The walls of the well occur at the lattice spacing. Such figures have been previously discussed by Mahan.[21] The electrostatic compression reduces the anion[21,22] polarizability; for F^- in LiF the Hartree-Fock polarizability is reduced from the free ion value of 10.65 to 7.30 a.u.[10]

In a real crystal the electrons are additionally compressed by overlap interactions with neighboring ions. This effect may be regarded as a property of a one-electron pseudopotential,[21] which may also be represented as in Eq. (4). For the same reasons as above the V_0 part of the pseudopotential will exert the dominant role and, because of the short range of overlap effects may also be thought of as a spherical potential well. The walls of the overlap well occur at a smaller radius than the electrostatic ones, at about the anion crystal radius (where the cation electron density becomes appreciable). The walls of the overlap well will therefore screen those of the electrostatic well when both effects are operating (see Sec. 7 of Ref. 18). The overlap compression of the F^- ion in LiF further reduces the F^- polarizability to 5.4 a.u..[10]

This simple idea of representing both overlap and electrostatic effects as a confining potential underlies the use of the charged "Watson sphere" to simulate the ionic environment. In its original form[23] the spherical well had a radius equal to the lattice spacing and a charge chosen to reproduce the Madelung potential inside, but in later applications a sphere of radius equal to the anionic radius has been used to simulate overlap effects.[20]

The analysis of the permittivity through the CM equation can only give information on the interactions between molecules which are occupying their equilibrium positions (i.e., on lattice sites for the crystal). For van der Waals materials this is already a good indication of how to model the fluctuating parts of the polarization (due to the displacement of particles from the lattice in a crystal) observed in light scattering as, in this case, the permittivity considerations show that it is a good approximation to neglect the $\vec{R}^N$ dependence of $\overleftrightarrow{\alpha}^i$.[7,24] Equations (1) and (2) then give an explicit expression for the $\vec{E}^0$-induced polarization as a function of the particle coordinates, which is found to account semiquantitatively for the shape and intensity of the Rayleigh wing in (for example) liquid argon.[25] For ionic crystals, although the static permittivity considerations suggest that the localized electron description is adequate, the large difference between the in crystal and free anion polarizabilities shows that the ionic polarizability depends strongly on the position of the other ions. For a description of the fluctuating polarization, Eqs. (1) and (2) are therefore incomplete without a prescription for this position dependence.

The simplest conceivable description of the fluctuating polarization in an ionic system would be to replace the $\vec{R}^N$-dependent ionic properties $\vec{\mu}^i(\vec{R}^N)$ and $\overleftrightarrow{\alpha}^i(\vec{R}^N)$ by their values in the undistorted crystal. Equations (1) and (2) are then complete. It does not take long to see, however, that the resulting description is hopelessly inadequate. The light-scattering spectrum, for example, will be simply that predicted by the dipole-induced dipole (DID) model (as in argon). The first-order DID model predicts a frequency-independent depolarization ratio of 0.75 for the Rayleigh wing,[7] whereas observations on molten salts show strongly frequency-dependent ratios which become as low as 0.1.[1-3]

At the next level of sophistication it is noted that in a perfect cubic lattice the first three gradients of the Coulomb potential vanish at an ionic position (lattice site), whereas in an instantaneous configuration of a distorted crystal or melt they do not. If we expand the ionic dipoles, quadrupoles and polarizabilities in powers of these distortion-induced gradients, we obtain:[26]

$$\mu^i_\alpha=\alpha F_\alpha+\tfrac{1}{6}\gamma_{\alpha\beta\gamma\delta}F_\beta F_\gamma F_\delta+\cdots+\tfrac{1}{2}B_{\alpha\beta,\gamma\delta}F_\beta F_{\gamma\delta}+\cdots+\tfrac{1}{10}E_{\alpha,\beta\gamma\delta}F_{\beta\gamma\delta}+\cdots, \tag{5}$$

$$\theta^i_{\alpha\beta}=\tfrac{1}{2}B_{\alpha\beta,\gamma\delta}F_\gamma F_\delta+\cdots+\tfrac{3}{2}C_{\alpha\beta,\gamma\delta}F_{\gamma\delta}+\cdots, \tag{6}$$

$$\alpha^i_{\alpha\beta}=\alpha\delta_{\alpha\beta}+\tfrac{1}{2}\gamma_{\alpha\beta\gamma\delta}F_\gamma F_\delta+\cdots+\tfrac{3}{4}B_{\alpha\beta,\gamma\delta}F_{\gamma\delta}+\cdots, \tag{7}$$

where α, B, C, E, γ are *in-crystal* values of the polarizabilities defined by these expressions and F_α, $F_{\alpha\beta}$, and $F_{\alpha\beta\gamma}$ are the first three gradients of the Coulomb potential evaluated at the site of ion i. If these expansions are truncated at low order [say that explicitly indicated in Eqs. (5)—(7)], then they provide, with Eqs. (1) and (2), explicit expressions for the interaction-induced polarization. The field and its gradients are readily evaluated from the ionic positions

$$F_{\alpha\beta\cdots\nu}(\vec{r}^{\,i})=\sum_{j\,(\neq i)}q^j T_{\alpha\beta\cdots\nu}(\vec{r}^{\,ij}) \tag{8a}$$

with

$$T_{\alpha\beta\ldots\nu}(\vec{r})=\nabla_\alpha\nabla_\beta\cdots\nabla_\nu r^{-1} \tag{8b}$$

and q^j the charge on ion j. Referring to the light-scattering problem discussed above we see that the hyperpolarization term in Eq. (5) provides a polarized contribution to the fluctuating polarization of the form

$$\delta P_\alpha=\sum_i \tfrac{1}{2}\gamma_{\alpha\beta\gamma\delta}F_\beta F_\gamma E^0_\delta \ . \tag{9}$$

This may therefore be partially responsible for the observed departure from the constant 0.75 depolarization ratio of the DID model. This mechanism has been invoked by Mazzacurati *et al.*[1] to account for the light scattering in AgI. The role of the B term in Eq. (5) has not been previously discussed; since B is traceless [i.e., $B_{\alpha\alpha,\gamma\delta}F_{\gamma\delta}=0$, Ref. 26)], this term will lead only to depolarized light scattering [in lowest order in Eq. (2)].

Equations such as (5)—(7) should suffice to describe the moment on ion i induced by fluctuations in the positions of ions at large distances from i. For such distant ions overlap effects should disappear and the convergence of the expansion in the gradients of the Coulomb potential should be rapid. Furthermore, the long-range fluctuations will tend to screen each other which will limit the size of the instantaneous field at any ion and ensure rapid convergence of the expansion in powers of the field and its gradients. For these reasons we shall refer to the model for the fluctuating polarization which follows from Eqs. (1) and (2) and (5)—(7) (truncated at the order explicitly indicated) as the "asymptotic model," as it correctly gives the contributions to the polarization due to interactions between ions separated by large distances.

The asymptotic model cannot be sufficient to describe the effect on the properties of an ion of fluctuations in the positions of near neighbors. For near neighbors overlap effects, neglected in Eqs. (5)—(7), become significant, as shown by the overlap compression effect on the in-crystal polarizability.[10,18] Furthermore, the expansion of the ionic properties in the gradients of the Coulomb potential fails to converge when the charges which cause the potential are at distances accessible to the electrons of the ion.[26]

In the present paper we wish to characterize the discrepancies between the predictions of the asymptotic model and the results of *ab initio* electronic structure calculations of the properties of an F^- ion in a *distorted* LiF lattice. The objective is to provide a treatment of the fluctuating polarization responsible for light scattering which includes both the asymptotic effects and the discrepancies.

We begin by presenting (in Sec. III) the results of calculations in which all neighbors of a central F^- ion are represented as point charges (called CRYST calculations) and the ions of the first shell of neighbors are radially distorted. Comparison of these results with the asymptotic model allows us to determine the effect of nonconvergence of the gradient expansion in Eqs. (5)—(7).

We then (in Sec. IV) introduce the overlap compression effects for the same distorted geometries, by representing the nearest neighbors of the central ion as full ions (i.e., nuclei plus electrons), while retaining the point-charge description of more distant particles. These are denoted CLUS calculations. In Sec. V, we consider the effects of tangential displacements of the first shell at both the CRYST and CLUS levels. We then consider how rapidly the distortion-induced properties converge to the asymptotic prediction as the distance between the central and displaced ions is increased (Sec. VI). Finally, we summarize our results and show how they may be used to define a computationally tractable set of equations for the fluctuation-induced polarization observed in light scattering.

III. POINT-CHARGE CALCULATIONS ON FIRST-SHELL DISTORTIONS

In this section we shall describe the results of calculations at the coupled Hartree-Fock level on the dipole moment, quadrupole moment, and polarizability of a fluoride ion in a simple cubic lattice of point charges with a lattice constant appropriate to LiF ($R=3.7965$ a.u.).[27] Except for the fact that some of the charges are now displaced from their lattice sites (see below) the calculations are identical to those described in Ref. 10 (denoted CHF-XTAL) and Ref. 18 (denoted CHF-CRYST). In particular, the same basis set is used for the F^- ion as in Ref. 10, this large [12s/8p/5d] set gives a polarizability for the free ion which is very close to the Hartree-Fock limit.

We are interested in comparing the results of the purely electrostatic environmental effects, which are all that occur in the CRYST calculations, with the predictions of the asymptotic model, described in Sec. II. For this we require values for the various polarizabilities which appear in Eqs. (5)—(7), calculated in the *undistorted* point-charge lattice, and in the same basis set as will be used in the distorted-lattice calculations. These polarizabilities may be calculated by methods we have described elsewhere[28] and their values are listed in Table I.

In this section we shall consider the results for radial displacements of one or two ions in the first coordination shell; these geometries are specified in Table II. Δ_1 and Δ_2 are the radial displacements of the charges at $+R$ and $-R$ along the z axis. The table also contains the value of the independent components of the first three gradients of the Coulomb potential at the fluoride ion for these geometries.

Tables III—VI give the *ab initio* results for the dipole moment, quadrupole moment, and the changes in the iso-

TABLE I. CRYST polarizabilities (a.u.) for the fluoride ion in the [12s 8p 5d] basis.

α	7.300
$C_{zz,zz}$	5.394
$C_{xz,xz}$	4.013
$B_{zz,zz}$	−96.0
γ_{zzzz}	679
γ_{xxzz}	141
$E_{z,zzz}$	2.95
$E_{x,xzz}$	−1.48

TABLE II. The distorted geometries at which calculations were carried out and the fields and field gradients at the F^- ion. Numbers in parentheses signify powers of 10; e.g., $1.792(-3)=1.792\times10^{-3}$.

Configuration no.	Δ_1 (a.u.)	Δ_2 (a.u.)	F_z (a.u.)	F_{zz} (a.u.)	F_{zzz} (a.u.)
1	0.05	0.05	0	2.814(−3)	0
2	0.05	0.0	1.792(−3)	1.407(−3)	1.473(−3)
3	0.1	0.1	0	5.485(−3)	0
4	0.1	0.0	3.515(−3)	2.742(−3)	2.853(−3)
5	0.5	0.5	0	2.2665(−2)	0
6	0.5	0.0	1.5208(−2)	1.1333(−2)	1.1274(−2)

tropic ($\alpha_1=\frac{1}{3}\,\mathrm{tr}\vec{\vec{\alpha}}-\alpha_{F^-}$) and anisotropic ($\alpha_2=\alpha_{zz}-\alpha_{xx}$) components of the polarizability induced by the distortion of the environment. These are compared with the predictions of the asymptotic model, i.e., for the axially symmetric distortions considered here:

$$\mu_z=\alpha F_z+\tfrac{1}{6}\gamma_{zzz}F_z^3+\tfrac{1}{2}B_{zz,zz}F_zF_{zz}+\tfrac{1}{10}E_{z,zzz}F_{zzz}\ , \tag{5'}$$

$$\theta_{zz}=\tfrac{1}{2}B_{zz,zz}F_z^2+\tfrac{3}{2}C_{zz,zz}F_{zz}\ , \tag{6'}$$

$$\alpha_1=\tfrac{1}{6}(\gamma_{zzz}+2\gamma_{xxzz})F_z^2\ , \tag{10}$$

$$\alpha_2=\tfrac{1}{2}(\gamma_{zzz}-\gamma_{xxzz})F_z^2+\tfrac{3}{4}B_{zz,zz}F_{zz}\ . \tag{11}$$

The contributions of the various terms in these equations to the total predicted by the model have been separately given in the tables in an obvious notation. The last columns of Tables III—VI give the value of the discrepancy ($\delta\mu_z$, etc.) between the *ab initio* value and that predicted by the asymptotic model.

Several observations can be made immediately about these results. The first is that the predicted and calculated values differ markedly. Second, we note that the discrepancies have the opposite sign to the asymptotic prediction and are largest for the properties which are most influenced by the outermost part of the electron density. Thus for the dipole moment, which is the first moment of the ground-state electron density, the discrepancy ($\delta\mu_z$) amounts to −22% of the predicted value (for geometry 2), whereas for the quadrupole, which is a second moment, it is −44%. The polarizability components are even more sensitive to the outer electron configuration (see Ref. 18, Table XIII); for the anisotropy the discrepancy is −65% of the predicted value.

The behavior of the discrepancies can be correlated rather well by considering the effects of geometric distortion on the electrostatic potential discussed in the last section. As we argued there the $l=4$ and higher-order parts of this potential do not affect the ionic polarizability; when the lattice is distorted new low-l components of V may be introduced. The distortion-induced changes in the potential, including terms up to $l=3$, are illustrated in Figs. 3 and 4 for an octahedron of point charges distorted as 2, 4, and 6 (Table II), but with $\Delta=R/10$. Figure 3 may be compared with Fig. 1 and the dashed contour is the lowest-energy contour of that figure which may be taken to represent the position of the electrostatic wall in the undistorted case, it has a radius equal to the lattice constant. Projections of the distorted and undistorted potentials along the z axis are shown in Fig. 4. To see which aspects of the distortion-induced changes in the electron density are accounted for by the asymptotic model, we also show in Fig. 4 the asymptotic potential

$$V_a(r)=V_0(r)+r_\alpha F_\alpha+\tfrac{1}{2}r_\alpha r_\beta F_{\alpha\beta}+\tfrac{1}{6}r_\alpha r_\beta r_\gamma F_{\alpha\beta\gamma}\ , \tag{12}$$

where V_0 is the spherical part of the undistorted potential and F_α, $F_{\alpha\beta}$, $F_{\alpha\beta\gamma}$ are components of the distortion-induced field and its first two gradients at the position of the central ion.

The figures show that the asymptotic potential is parallel to the distorted potential *inside* the original electrostatic potential well (i.e., for $r<R$). For larger values of r the actual potential lies below the asymptotic potential (for positive z) *and* below the undistorted potential. The situation may be summarized by describing the actual potential as the sum of the asymptotic potential and a distortion-induced "dent" in the confining wall of the electrostatic potential well whose origins we discussed in the last section. The discrepancy between the calculated properties and the predictions of the asymptotic model may then be ascribed to the effects of this dent.

The asymptotic potential of Fig. 4 (corresponding to geometries 2, 4, and 6) favors a displacement of electrons to negative z and a positive value for the distortion-induced dipole. The dent in the wall gives rise to a flow of electrons to positive z which will therefore tend to

TABLE III. Calculated and predicted values of the CRYST dipole moment (for configuration 1, 3, and 5 the calculated and predicted values are zero).

		μ_z (predicted)					
Configuration no.	μ_z (calc)	α	γ	B	E	Total	$\delta\mu_z$
2	1.053(−2)	1.308(−2)	0.7(−7)	1.213(−4)	4.344(−4)	1.339(−2)	−2.87(−3)
4	2.073(−2)	2.566(−2)	0.49(−6)	4.628(−4)	8.415(−4)	2.605(−2)	−5.32(−3)
6	9.161(−2)	1.1102(−1)	3.981(−4)	8.273(−3)	3.326(−3)	1.0648(−1)	−1.486(−2)

TABLE IV. Calculated and predicted values of the CRYST quadrupole.

Configuration no.	θ_{zz} (calc)	θ_{zz} (predicted) B	C	Total	$\delta\theta_{zz}$
1	1.267(−2)	0	2.276(−2)	2.276(−2)	−1.010(−2)
2	6.235(−3)	−1.54(−4)	1.138(−2)	1.123(−2)	−4.99(−3)
3	2.508(−2)	0	4.438(−2)	4.438(−2)	1.930(−2)
4	1.252(−2)	−5.93(−4)	2.219(−2)	2.219(−2)	−9.07(−3)
5	1.1451(−1)	0	1.8339(−1)	1.8339(−1)	−6.89(−2)
6	4.920(−2)	−1.110(−2)	9.169(−2)	8.594(−2)	−3.68(−2)

reduce the value of the dipole from the asymptotic prediction.

The distortion-induced quadrupole may be described in the same way. Consider a simultaneous outward movement of the charges at $z=\pm R$ in an octahedral array (as in geometries 1, 3, and 5). This produces a potential whose contours are illustrated in Fig. 5, the potential wall now has two dents. Recall that

$$\theta_{zz}=\tfrac{1}{2}\sum_{i\ (\text{electrons})}\langle r_i^2\rangle-3\langle z_i^2\rangle\ , \tag{13}$$

so that a flow of electrons into the dents at $+$ and $-z$ produces a negative contribution to θ_{zz}, again opposing the prediction of the asymptotic model. We expect the quadrupole to be more sensitive than the dipole to the change in the confining wall, and the quadrupole discrepancy to be correspondingly larger, as it is more sensitive to the outermost part of the electron density, which is where the dent in the confining wall is effective.

The Kirkwood approximation[29]

$$\alpha_{aa}=(4/n)\sum_i\{\langle r_{ai}^2\rangle\}^2 \tag{14}$$

(where n is an effective number of electrons) may be used to relate the changes in the polarizability to the changes in the extent of the electron cloud. It suggests immediately that the polarizability will be more sensitive than the quadrupole moment and the discrepancies correspondingly larger. Furthermore, on the basis of the dent in the wall picture we expect $\langle r_{zi}^2\rangle$ to increase while $\langle r_{\xi}^2\rangle$ and $\langle r_{yi}^2\rangle$ remain constant (this is borne out by the calculations). We therefore expect that the discrepancy ($\delta\alpha_1$) in the isotropic polarizability will be about one third of the discrepancy in the anisotropic polarizability. This expectation is quite accurately supported by the results.

These considerations suggest that the picture of an in-crystal anion as confined in a spherical potential well may be usefully extended for understanding the distortion-induced properties. The asymptotic model would give correctly the distortion-induced properties if the central ion were a polarizable *point*. The dent in the wall picture corrects this prediction for the extended distribution of polarizable matter in the actual ion. It is perhaps worth reemphasizing that the only environmental effects in these CRYST calculations are electrostatic in origin. A model

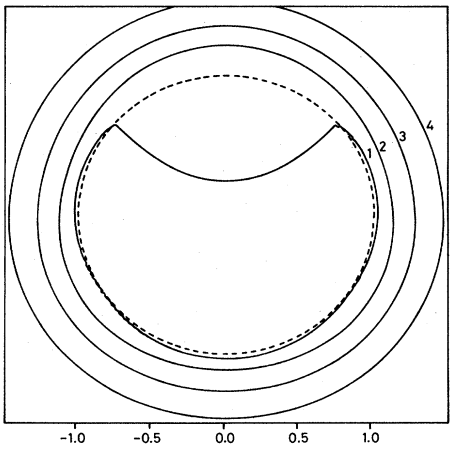

FIG. 3. Potential energy of an electron in a dipolar distortion of an octahedral array. The charge at $z=R$ has been displaced to 1.1R. The figure is a slice through the xz plane with $-3/2R\le x,z\le 3/2R$. Contours counting out from the center at 0.974ϵ, 0.875ϵ, 0.775ϵ, 0.675ϵ. The dotted circle is the contour of the undistorted potential (Fig. 1). Spherical components up to $L=3$ are included in the potential.

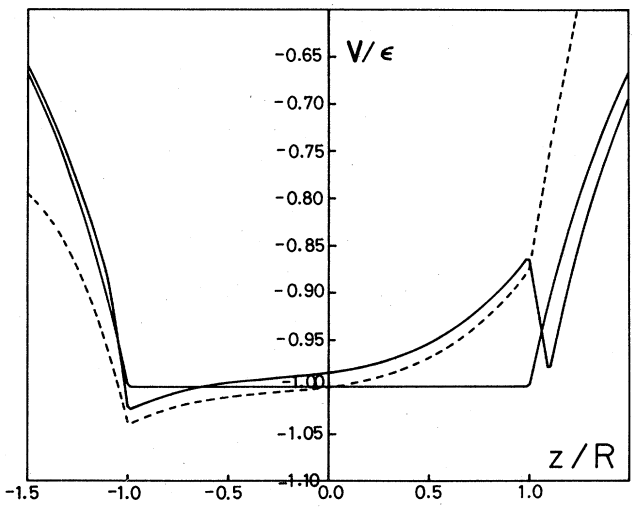

FIG. 4. Potential energy of an electron in a dipolar distortion of an octahedral array. The graph is a section along the z axis of Fig. 3. The extra curves are the spherical potential of the undistorted array (Fig. 2) and the asymptotic potential (dotted line).

TABLE V. Calculated and predicted values of the CRYST polarizability anisotropy.

Configuration no.	$(\alpha_{zz}-\alpha_{xx})$ (calc)	$(\alpha_{zz}-\alpha_{xx})$ (predicted) B	γ	Total	$\delta\alpha_2$
1	−7.135(−2)	−2.0258(−1)	0	−2.0258(−1)	1.3123(−1)
2	−3.535(−2)	−1.0129(−1)	8.64(−4)	−1.0042(−1)	6.507(−2)
3	−1.426(−1)	−3.9490(−1)	0	−3.9490(−1)	2.5228(−1)
4	−7.007(−2)	−1.9745(−1)	3.32(−3)	−1.9413(−1)	1.2406(−1)
5	−6.967(−1)	−1.63192(0)	0	−1.63192(0)	9.3525(−1)
6	−3.188(−1)	−8.1596(−1)	6.22(−2)	−7.5374(−1)	4.3490(−1)

of the real crystal must also incorporate the effects of overlap.

IV. FIRST-SHELL EFFECTS INCLUDING OVERLAP

The effect of first-shell overlap compression on the distortion-induced properties of the fluoride ion may be evaluated from the values of these properties for a distorted cluster of an F^- ion surrounded by six Li^+ neighbors in a lattice of point charges. Although we calculate the property for the cluster as a whole we are interested in decomposing this result to obtain the environmental effect on the property for the F^- ion. In Refs. 10 and 18 we described how the overlap compression effect on the in-crystal polarizability could be found from such CLUS calculations when the Li^+ ions were disposed on a regular octahedron defined by the first neighbor lattice sites. Here we give the results when the octahedron suffers the same distortions as specified in Table II; the *electrostatic* perturbations of the central ion are thus the same as in the last section, except that the nearest-neighbor ions are now charge distributions rather than points.

As discussed in Refs. 10 and 18, a satisfactory representation of the in-crystal Li^+ ion, at the Hartree-Fock level, can be accomplished with just two orbitals. These orbitals (of $[s]$ and $[p]$ type) are constructed from a large $(10s,5p)$ basis so as to give the Hartree-Fock ground-state wave function $[s]^2$ and the first-order perturbed wave function in the presence of a uniform externally applied field $[sp]$. The ground-state electron density, energy, and polarizability in this small basis are therefore the same as those calculated with the uncontracted $(10s,5p)$ set, and very close to the Hartree-Fock limit.

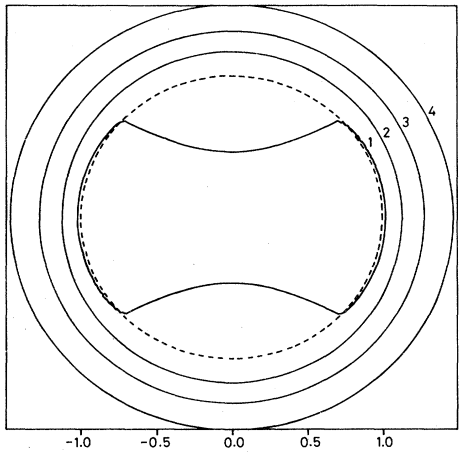

FIG. 5. Potential energy of an electron in a quadrupolar distortion of an octahedral array. As Fig. 3, except that *both* charges at $z=\pm R$ have been displaced to $\pm 1.1R$.

The extraction of the environmental effect on the value of a property of the F^- ion from the value of the property of the F^- ion from the value of the property for the whole cluster depends upon the fact that the electron density of the Li^+ ion is extremely insensitive to its environment. Furthermore, with the basis sets we are using (see also Ref. 10), the contributions to the calculated properties from basis set superposition error[30] is very small, as we shall show below. We may therefore write (taking the polarizability as an example)

$$\overleftrightarrow{\alpha}_{\mathrm{CLUS}}(F^-,6\,Li^+)=\overleftrightarrow{\alpha}_{\mathrm{CLUS}}(6\,Li^+)+\overleftrightarrow{\alpha}_{\mathrm{DID}}(F^-,6\,Li^+)+\overleftrightarrow{\alpha}_{\mathrm{INT}}(F^-,6\,Li^+)\,, \tag{15a}$$

where $\overleftrightarrow{\alpha}_{\mathrm{CLUS}}(F^-,6\,Li^+)$ is the directly calculated polarizability of the distorted cluster described above. $\overleftrightarrow{\alpha}_{\mathrm{CLUS}}(6\,Li^+)$ is the independently calculated polarizability of an identically distorted cluster in which the central F^- ion is replaced by a point charge. Because the environmental effects on Li^+ are so small, we expect that the contribution to the polarizability of the $(F^-,6Li^+)$ cluster arising from the Li^+ ions and from the Li^+-Li^+ interactions is the same as the polarizability of the distorted $6Li^+$ cluster.[10] $\overleftrightarrow{\alpha}_{\mathrm{DID}}(F^-,6Li^+)$ contains the contributions to the cluster polarizability which arise from dipole-induced dipole interactions between the fluoride ion and the Li^+ ions, i.e., from the interion terms which arise when Eqs. (1) and (2) are iterated [note that the Li^+-Li^+ DID terms are contained within $\overleftrightarrow{\alpha}_{\mathrm{CLUS}}(6Li^+)$]. The DID terms are given by

TABLE VI. Calculated and predicted values of the isotropic CRYST polarizability.

Configuration no.	$\frac{1}{3}\mathrm{tr}\overleftrightarrow{\alpha}$ (calc) $-\alpha_{F^-}$	$\frac{1}{3}\mathrm{tr}\overleftrightarrow{\alpha}$ (predicted) $\gamma\equiv$total	$\delta\alpha_1$
1	3.779(−2)	0	3.779(−2)
2	1.875(−2)	5.14(−4)	1.823(−2)
3	7.417(−2)	0	7.417(−2)
4	3.653(−2)	1.98(−3)	3.455(−2)
5	3.2169(−1)	0	3.2169(−1)
6	1.4929(−1)	3.70(−2)	1.129(−1)

$$[\vec{\alpha}_{\mathrm{DID}}(F^-,6Li^+)]=2\alpha_{F^-}\alpha_{Li^+}\sum_{j=1}^{6}T_{\alpha\beta}(\vec{r}_j)$$
$$+(\alpha_{F^-})^2\alpha_{Li^+}\sum_{j=1}^{6}T_{\alpha\gamma}(\vec{r}_j)T_{\gamma\beta}(-\vec{r}_j)$$
$$+O(\alpha_{F^-}(\alpha_{Li^+})^2)\ . \qquad (15b)$$

The polarizabilities are the nominal (CLUS) in-crystal polarizabilities and r_j is the position of the jth Li^+ ion from the fluoride ion. The DID term of order $\alpha_{F^-}(\alpha^+_{Li^+})^2$ (and higher-order terms) may be neglected because of the small value of the Li^+ polarizability compared to that of F^-. Since (as we show below) basis-set superposition errors are negligible, α_{INT} contains the effect of overlap compression as well as the electrostatic crystal field effects which were separately studied in the last section.

We again wish to compare the predictions of the asymptotic model [i.e., Eqs. (5)—(7)] with the calculated distortion-induced properties of the F^- ion. However, for this we need values for the ionic hyperpolarizabilities (γ, β) etc.) for the undistorted CLUS environment; these differ from the CRYST values used in the last section because they are affected by overlap compression. We have recently calculated values for these quantities[28] using the same basis sets as employed here, they are reproduced in Table VII. (Note that while the values given here are useful for the present calculation, they are not expected to accurately represent the true properties of F^- because of the limitations of the *spd* basis; calculations in an extended basis are also discussed in Ref. 28.)

Tables VIII—XI show the comparison between the calculated values of the dipole moment, quadrupole moment and the isotropic and anisotropic parts of the polarizability, and the values predicted by the asymptotic model. The calculated quantity presented in the table is the difference between the value calculated for the F^-6Li^+ cluster and the $6Li^+$ cluster, it therefore contains the DID contributions. We have estimated the basis-set superposition error contribution to these results by performing subsidiary calculations in which the basis functions of the F^- ion are retained (but not the electrons). The difference between the properties obtained in these calculations and those found for the simple $6Li^+$ cluster should give an upper bound (cf. Ref. 10) to the superposition errors in the full results. These considerations show that even in the worst case (the quadrupole moment), the basis-set superposition errors in the calculated values which appear in the table do not exceed 1%; in the other cases the errors are considerably smaller. The only property for which the DID contribution exceeds 1% is the polarizability anisotropy, in other cases this has been omitted from the tables.

TABLE VII. CLUS polarizabilities (a.u.) for the fluoride ion in the [12*s* 8*p* 5*d*]/[1*s*/1*p*] basis.

$\alpha_{F^-}=5.40$
$\alpha_{Li^+}=0.192$
$\gamma_{zzzz}=149.0$
$B_{zzzz}=-34.5$
$E_{z,zz}=4.1$
$C_{zz,zz}=4.39$

The discrepancies between the predictions of the asymptotic model and the *ab initio* results show many similarities with those found in the CRYST calculations. The discrepancies have the opposite sign to the asymptotic predictions and the sizes of the discrepancies relative to the predictions of the asymptotic model are again smallest for the dipole and largest for the polarizability. For geometry 2 the discrepancies are −65% (dipole), −103% (quadrupole), and −146% (α_2) of the asymptotic predictions, each about twice the CRYST discrepancy. As in the CRYST case the discrepancy in the anisotropic polarizability (α_2) is about three times larger than that in the isotropic polarizability (α_1).

These similarities suggest a rationalization of the CLUS results by extending the concept of the "dent in the confining wall", which we introduced in the last section. As discussed in Sec. II, overlap compression may be considered as the result of a pseudopotential well with walls which rise steeply at the anionic radius. Outward movement of one of the first shell cations produces a dent in this pseudopotential wall, analogous to and in the same sense as that in the electrostatic wall which we demonstrated in Sec. III, so that the above-mentioned observations may be readily rationalized. Because the overlap well is of smaller radius than the electrostatic well a given displacement of the wall will produce a larger relative effect—as noted above.

V. CALCULATIONS ON FIRST-SHELL BENDING DISPLACEMENTS

In the two previous sections we have considered the effect of radial displacements of Li^+ ions in the first coordination shell; here we consider first-shell tangential displacements. Calculations have been carried out on two distorted configurations (7 and 8) which are displayed in

TABLE VIII. Calculated and predicted values of the CLUS dipole moment. The γ contributions to μ are smaller than the superposition errors and have been neglected.

Configuration no.	μ_z (calc)	μ_z (predicted) α	B	E	Total	$\delta\mu_z$
2	3.637(−3)	9.68(−3)	4.3(−5)	6.0(−4)	1.03(−2)	−6.7(−3)
4	7.387(−3)	1.899(−2)	1.66(−4)	1.17(−3)	2.03(−2)	−1.29(−2)

TABLE IX. Calculated and predicted values of the CLUS quadrupole moment. The B contribution is smaller than the superposition errors and has been neglected.

Configuration no.	θ_{zz} (calc)	θ_{zz} (predicted)	$\delta\theta_{zz}$
1	−1.515(−3)	1.857(−2)	−2.008(−2)
2	−7.42(−4)	9.17(−3)	−9.91(−3)
3	−2.709(−3)	3.620(−2)	−3.891(−2)
4	−1.294(−3)	1.762(−2)	−1.891(−2)

Fig. 6. It can be shown by a symmetry-coordinate analysis of the displacements of the first neighbor shell in the group O_h that the geometries 1, 2, 3, 4, 7, and 8 span the distortions which, by symmetry considerations, may activate the dipole moment (T_{1u}), polarizability (A_{1g}, E_g, T_{2g}), and quadrupole moment (E_g, T_{2g}) of the fluoride ion on its lattice site.

For geometry 7 the asymptotic model predicts

$$\alpha_{xy}=\tfrac{2}{3}B_{xy,xy}F_{xy}\ , \tag{16}$$

$$\theta_{xy}=2C_{xy,xy}F_{xy}\ , \tag{17}$$

and

$$F_{xy}=-5.768\times10^{-3}ea_0^{-3}\ . \tag{18}$$

For geometry 8 the distortion-induced dipole moment is given by

$$\mu_z=\alpha F_z+O((\Delta/R)^3) \tag{19}$$

and

$$F_z=-6.940\times10^{-3}ea_0^{-2}\ , \tag{20}$$

where, in each case, the displaced ions have moved 0.1 bohr off their lattice sites.

CRYST calculations have been carried out on geometries 7 and 8. The results are compared with the predictions of the asymptotic model [from Eqs. (16)—(20) using the polarizabilities given in Table II] in Table XII.

The discrepancies between the calculated and predicted values are much smaller than for radial displacements of the same amplitude, they are −4% (dipole), −18% (quadrupole), and −29% (polarizability) of the asymptotic prediction. It would be expected from the distorted well ideas that the asymptotic model would be relatively successful for tangential displacements as the confining well is much less distorted than by a radial displacement of the same amplitude.

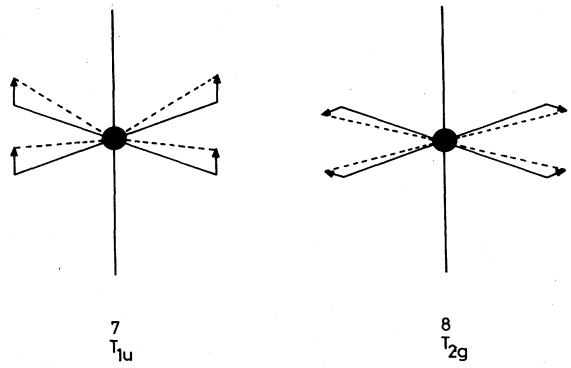

FIG. 6. Bending distortions of the octahedron. Geometries 7 and 8 are illustrated.

At a more detailed level the change in the shape of the confining wall can account for the sign of the discrepancy of the polarizability and quadrupole moment. Figure 7 shows the contours of the distorted potential for a pure bending T_{2g} distortion of an octahedron in which each of the charges in the x,y plane moves through 3°. The asymptotic potential rises quadratically (with respect to the undistorted potential) along the $(\pm x',y'=0)$ axis and decreases quadratically along $(x'=0,\pm y')$, where $x'=2^{-1/2}(x+y)$ and $y'=2^{-1/2}(x-y)$. The quadrupole and polarizability are related to the moments of the electron density in the x',y' frame by

$$\theta_{xy}=-\sum_i[\langle(x_i')^2\rangle-\langle(y_i')^2\rangle] \tag{21}$$

and (Kirkwood approximation)

$$\alpha_{xy}\simeq(4/n)\sum_i[\langle(x_i')^2\rangle^2-\langle(y_i')^2\rangle^2]\ , \tag{22}$$

so that the asymptotic predictions are, respectively, negative and positive. Inside the circle of radius R the asymptotic potential agrees with the true one, but outside it overestimates the difference between the distorted potential and V_0. The difference between the true potential and the asymptotic one (i.e., the dent in the wall potential) corresponds to an outwards movement of the wall along $\pm y'$ and an inwards movement along $\pm x'$. The dent is therefore responsible for an increase in $\langle(y')^2\rangle$ and a decrease in $\langle(x')^2\rangle$, relative to the values of these quantities with the asymptotic potential, and consequently to positive and negative discrepancies in the quadrupole and polarizability, respectively.

TABLE X. Calculated and predicted values of the CLUS polarizability anisotropy. The γ contributions are less than the superposition error and have been omitted.

Configuration no.	$(\alpha_{zz}-\alpha_{xx})$ (calc)	$(\alpha_{zz}-\alpha_{xx})$ (predicted) DID	B	$\delta\alpha_2$
1	2.508(−2)	−8.71(−3)	−7.28(−2)	1.066(−1)
2	1.237(−2)	−4.36(−3)	−3.61(−2)	5.29(−2)
3	4.866(−2)	−1.710(−2)	−1.419(−1)	2.076(−1)
4	2.373(−2)	−8.53(−3)	−6.98(−2)	1.020(−1)

TABLE XI. Calculated values of the CLUS isotropic polarizability. Both the γ and second-order DID contributions are of the same size as the superposition errors and are neglected.

Configuration no.	1
1	3.835(−2)
2	1.907(−2)
3	7.548(−2)
4	3.729(−2)

We have also carried out a single CLUS calculation on geometry 8, in order to check the effect of overlap on the properties induced by bending displacements. After analysis in the usual way [cf. Eq. (15) and the subsequent discussion], the induced properties were found to be

$$\alpha_{xy} = +0.0416 \text{ a.u. (CLUS)}, \tag{23}$$

$$\theta_{xy} = -0.0157 \text{ a.u. (CLUS)}. \tag{24}$$

DID and BSSE corrections to these properties were negligible. The asymptotic predictions [Eqs. (16)–(18)] require values for $C_{xy,xy}$ and $B_{xy,xy}$ for the CLUS ion. These are not available, but assuming that the degree of anisotropy in the CLUS and CRYST tensors is the same, i.e.,

$$C^{\text{CLUS}}_{xy,xy}/C^{\text{CRYST}}_{xy,xy} = C^{\text{CLUS}}_{xx,xx}/C^{\text{CRYST}}_{xx,xx} \tag{25}$$

and

$$B^{\text{CLUS}}_{xy,xy}/B^{\text{CRYST}}_{xy,xy} = B^{\text{CLUS}}_{xx,xx}/B^{\text{CRYST}}_{xx,xx}, \tag{26}$$

we can derive asymptotic predictions of

$$\alpha_{xy} = +0.079, \quad \delta\alpha_{xy} = -0.037, \tag{27}$$

$$\theta_{xy} = -0.040, \quad \delta\theta = 0.024. \tag{28}$$

Thus the discrepancies (relative to the predicted values) are both larger in magnitude (both are −47%) than in the CRYST calculations and of the same sign. This is to be expected from the change in shape of the overlap contributions to the confining wall. The change will favor the movement of electrons into the region vacated by the displaced cations, that is, $\langle (y')^2 \rangle$ will be increased and $\langle (x')^2 \rangle$ decreased. This is a change in the same sense as produced by the dent in the electrostatic wall responsible for the discrepancy in the CRYST results.

VI. SECOND- AND THIRD-SHELL DISPLACEMENTS

We have performed a limited series of CRYST calculations in which ions in the second shell (i.e., the first shell of anion neighbors at $\sqrt{2}R$) and the third shell (the second shell at $\sqrt{3}R$) are displaced from their lattice sites. These calculations were undertaken to examine how rapidly the purely electrostatic effects converge to the predictions of the asymptotic model as the distance between the displaced site and the central fluoride ion is increased.

TABLE XII. Calculated and predicted quantities for geometries 7 and 8.

Geometry	Property	Calculated	Predicted	Discrepancy
7	μ_z	−0.048 72	−0.050 66	0.001 94
8	α_{xy}	0.152 71	0.2153	−0.0626
8	θ_{xy}	−0.037 90	−0.046 29	+0.008 39

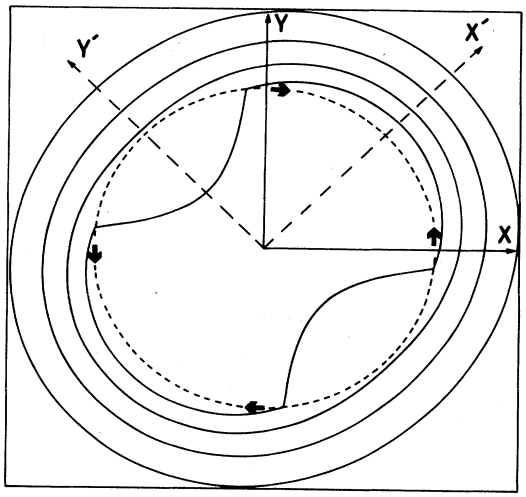

FIG. 7. Potential energy of an electron in a T_{2g} distorted octahedron. The figure is a slice through the x-y plane of a distortion like geometry 8, where each equatorial cation has moved through 3°. The short arrows show the cation displacements and full and dotted axes show the original and rotated principal axes of (see text). Contours as Fig. 3.

In the second shell, calculations were made with the charge at $(R,R,0)$ displaced to $(R+\Delta, R+\Delta, 0)$ with $\Delta = 0.035$ a.u. (geometry 9) and 0.070 a.u. (geometry 10). These displacements change the distance between this charge and the fluoride ion by 0.05 and 0.1 a.u., respectively, so that the magnitudes of the distortion-induced properties may be directly compared with geometries 2 and 4 of Table II. In the third shell the ion at (R,R,R) was displaced to $(R+\Delta, R+\Delta, R+\Delta)$ with $\Delta = 0.029$ a.u. (geometry 11) and $\Delta = 0.058$ a.u. (geometry 10) which again change the distance between this charge, and the central ion by 0.05 and 0.1 a.u. The resulting small displacement-induced properties of the F^- ion are given in Table XIII.

The asymptotic model [Eqs. (5) to (7)] has been used to predict the distortion-induced properties as in previous sections of this paper. As in the first shell CRYST calculations we find that for the dipole, quadrupole, and anisotropic polarizability the asymptotic prediction is opposed by an additional contribution of opposite sign. The origins of this discrepancy may be successfully rationalized by considering the change in the shape of the confining potential in the manner discussed above, that is the sign and magnitude of the discrepancy and the relationship between the discrepancy in different components of the same tensor may all be predicted. Consider, for example, the behavior of the components of the polarizability in

TABLE XIII. Properties induced by distortions in second and third shells in the point-charge model. Geometries 9 to 12 are defined in the text.

Property	Geometry 9	10	11	12
α_1	−1.507(−3)	−2.701(−3)	−2.11(−4)	−5.35(−4)
α_2	−1.010(−2)	−2.018(−2)	0	0
α_{xy}	+ 8.294(−3)	+ 1.649(−2)	−2.767(−3)	−5.432(−3)
μ_x	−3.168(−3)	−6.268(−3)	+ 1.447(−3)	+ 2.860(−3)
θ_{zz}	1.326(−3)	2.636(−3)	0	0
θ_{xy}	−1.970(−3)	−3.915(−3)	+ 6.24(−4)	+ 1.222(−3)

geometry 9. In the coordinate system which coincides with the principal axes of the distorted tensor,

$$(x',y',z') \equiv (2^{-1/2}(x+y),\ 2^{-1/2}(-x+y),z)\ ,$$

the discrepancies are

$$\delta\alpha_{x'x'} = -3.92(-3),\quad \delta\alpha_{y'y'} = -8.1(-4)$$

and

$$\delta\alpha_{z'z'} = 2.2(-4)\ ;$$

the discrepancy is thus predominantly in the x' component (i.e., along the line of the distortion). Outward movement of a negatively charged ion in the second shell creates a bump in the confining wall of the electrostatic potential (i.e., an *inward* movement of the wall), thus we expect $\langle (x')^2 \rangle$ to be decreased by this effect leading to a negative discrepancy.

As we shall argue below, the actual values of the electrostatic discrepancies are of limited significance. Far more important is the fact they they appear to be becoming small quite rapidly for displacements in the more distant coordination shells. As shown in Table XIV, where the percentage ratio of the discrepancy to the asymptotically predicted value for a radial displacement of a given size is given, by the time we reach the third shell the dipole, quadrupole, and anisotropic polarizability are well described by the asymptotic model. The single exception is the isotropic polarizability for which the asymptotic prediction is always extremely low; however, the absolute size of the third shell distortion-induced isotropic polarizability is itself very small (about 2% of the first shell effect).

We have not performed any calculations from which the overlap effects on the properties induced by second- and third-shell distortions may be evaluated. However the CLUS calculations described in previous sections enable us to arrive at some qualitative conclusions. It is useful to consider separately two aspects of the overlap problem. First, the overlap with the *first* shell ions will alter properties induced by second- and third-shell distortions through electrostatic interactions. The asymptotic contributions will be altered, because the distortion-induced fields act on the CLUS polarizability. Also the size of the electrostatic discrepancies calculated above will be reduced, because the first shell overlap effects will prevent the electrons of the anion from penetrating to the region $r > \sqrt{2}R$, which is where the dent in the confining electrostatic potential is active. We believe that the electrostatic discrepancies will become insignificant by virtue of this effect. Second, we refer to the influence of overlap with the second- and third-shell ions themselves. For the third shell such effects are unlikely to be large, because of the short range of the overlap interactions and the overlap compression by the first two shells. However, for the second shell overlap effects could be important, particularly when a large anion and a small cation are involved. For LiF we concluded,[10] because of the good agreement between the calculated in-crystal polarizability of F^- with the experimental value, that the second-shell overlap effects were much less important than the first-shell ones included in the CLUS calculations. As we have seen above (Sec. III—V), for first-shell distortions the overlap and electrostatic contributions to the discrepancy between calculation and asymptotic prediction act in concert. For the second shell this will not be so. For an outward displacement of an ion in the second shell the second-shell overlap effects will favor a movement of electrons in the direction of the displacement and consequently an increase in (for example) the component of the polarizability in this direction. As we have seen above the electrostatic discrepancy for this component is negative.

TABLE XIV. Convergence of electrostatic distortion-induced properties to the asymptotic limit. The figure shown is the discrepancy (calculated-asymptotic value) as a % of the asymptotic value for small radial displacements.

Property	Shell 1	Shell 2	Shell 3
α_2	65	20	
α_{xy}		16	6
μ	22	3	2
θ	44	7	2

VII. A MODEL FOR THE FLUCTUATING POLARIZATION

We have seen in the previous sections how the distortion-induced dipole, quadrupole, and polarizability of F^- in LiF can be satisfactorily attributed to two distinct mechanisms. The asymptotic model accounts for the polarization which would be induced if the anions were polarizable points, and the discrepancy between this model and reality may be assigned to the change in shape of the confining potential surrounding the anion, which is

TABLE XV. Analysis of properties induced by first-shell distortions in terms of symmetry coordinates. All properties in a.u. Symmetry coordinates are in bohr-radius units. Quantities in parentheses are estimated. CRYST and CLUS are the *ab initio* results and CRYST asym, CLUS asym are the asymptotic models at these levels. δ=CLUS−CLUS asym.

Derivative	CRYST	CRYST asym	CLUS	CLUS asym	δ
$(\partial\mu_z/\partial S_{3z})$	+0.302	+0.389	+0.101	+0.296	−0.195
$(\partial\mu_z/\partial S_{4z})$	−0.654	−0.680			
$(\partial\alpha_1/\partial S_1)$	+0.945	+0.002	+0.955	0.000	+0.955
$[\partial(\alpha_{xx}-\alpha_{zz})/\partial S_{2a}]$	−1.235	−3.594	+0.600	−1.292	+1.892
$(\partial\alpha_{xy}/\partial S_{5z})$	−1.450	−2.044	−0.395	(−0.75)	−0.320
$(\partial\theta_{zz}/\partial S_{2a})$	+0.213	+0.390	−0.029	0.330	−0.359
$(\partial\theta_{xy}/\partial S_{5z})$	+0.360	+0.439	+0.149	(+0.38)	−0.111

sensed by its distributed electron density. The confining potential is due to both electrostatic and overlap interactions. We have shown that for first-shell distortions both effects act in concert, but that overlap tends to dominate. The dent in the confining potential is the overwhelmingly dominant cause of the distortion-induced isotropic polarizability; this is supported by the early work of Hardy[31] who successfully calculated the polarized light scattering spectrum of crystalline NaF with a semiempirical model for the fluctuating polarizability which included only such effects. For first-shell distortions the asymptotic model is much more successful for bending than stretching motions. We have shown directly that the properties induced by second- and third-shell distortions via purely electrostatic interactions converge quite rapidly to the asymptotic model predictions. We also argued that overlap effects will tend to improve still further the asymptotic predictions outside the first shell.

We now turn to the problem of how to make use of these observations in building an explicit model for the fluctuating polarization which is computationally tractable within the context of a computer simulation. The most significant finding is that the asymptotic model appears to be reliable for all but first-shell distortions. This suggests that we build a computational scheme by supplementing the equations which prescribe the asymptotic predictions [i.e., Eqs. (5)—(7)] with additional terms which are operative only for the first shell of cations around an anion. The remaining problem is then to use our results to parametrize suitable expressions for the discrepancies between the first-shell distortion-induced properties we have calculated and the asymptotic model predictions.

The results that we have presented in Sec. IV and V for weakly distorted lattices enable us to specify the linear response of dipole moment, quadrupole moment, and polarizability with respect to local distortions from the perfect crystal lattice. One way to collect this information is in terms of symmetry coordinates of the $(F^-)(Li^+)_6$ cluster. These coordinates are defined in terms of r_i, the position vector of the ith Li^+ ion from the F^- origin and

$$\phi_{ij}=\cos^{-1}(\vec{r}_i\cdot\vec{r}_j/r_i r_j)$$

as the nonredundant set

$$S_1(A_{1g})=(1/\sqrt{6})(\delta r_1+\delta r_2+\delta r_3+\delta r_4+\delta r_5+\delta r_6)\ , \tag{29}$$

$$S_{2a}(E_g)=(1/\sqrt{12})(2\delta r_1+2\delta r_2-\delta r_3-\delta r_4-\delta r_5-\delta r_6) \tag{30}$$

$$S_{3z}(T_{1u})=(1/\sqrt{2})(\delta r_1-\delta r_2)\ , \tag{31}$$

$$S_{4z}(T_{1u})=(1/\sqrt{8})(\delta_{23}+\delta\phi_{24}+\delta\phi_{25}+\delta\phi_{26}-\delta\phi_{13}-\delta\phi_{14}-\delta\phi_{15}-\delta\phi_{16}) \tag{32}$$

$$S_{5z}(T_{2g})=\tfrac{1}{2}(\delta\phi_{35}-\delta\phi_{36}-\delta\phi_{45}+\delta\phi_{46}) \tag{33}$$

$$S_{6z}(T_{2u})=(1/\sqrt{8})(\delta\phi_{15}+\delta\phi_{16}+\delta\phi_{23}+\delta\phi_{24}-\delta\phi_{13}-\delta\phi_{14}-\delta\phi_{25}-\delta\phi_{26})\ . \tag{34}$$

A T_{1g} rotational redundancy has been removed.

Table XV lists the derivatives of the properties with these distortion coordinates. Each value is given at CRYST and CLUS levels with the asymptotic predictions at each level. The final column gives the discrepancy between the CLUS *ab initio* and asymptotic derivatives and is thus the effect of the dent in the wall mechanism on the property.

As an illustration of how the calculations in the present paper may be used to set up a model for computer simulation, we consider the fluctuating polarizability. For ease of evaluation the terms which supplement the asymptotic model should be written as sums of pair functions, each of which depends only on the distance between the central F^- and one Li^+ ion. A general representation of the discrepancy in the distortion-induced polarizability of a fluoride ion within this constraint is

$$\delta\alpha_{\alpha\beta}=\sum_{i\in S}[\delta_{\alpha\beta}a(r_i)+\tfrac{1}{2}(3r_{i\alpha}r_{i\alpha}-r_i^2\delta_{\alpha\beta})r_i^{-2}b(r_i)]\ , \tag{35}$$

where each pair contribution to $\delta\vec{\vec{\alpha}}$ is a symmetric second-rank tensor depending only on the interion vector $\vec{r}_i$. The sum runs over the six cations in the first shell around a fluoride ion. Noting that $\delta\vec{\vec{\alpha}}$ vanishes when all first-shell ions are on their lattice sites and using the definitions of the S_i with the δ column of Table XV, we find

$$a(R)=0\ ,$$

$$\left[\frac{\partial a}{\partial r}\right]_{r=R}=\frac{1}{\sqrt{6}}\frac{\partial\delta\alpha_1}{\partial S_1}=+3.9\times10^{-1}\ , \tag{36}$$

$$b(R)=-\frac{2}{3}\frac{\partial\delta\alpha_{xy}}{\partial S_{5z}}=+2.1\times10^{-1}\ , \tag{37}$$

$$\left[\frac{\partial b}{\partial r}\right]_{r=R}=\frac{1}{3\sqrt{3}}\frac{\partial\delta\alpha_2}{\partial S_{2a}}=-7.28\times10^{-1}\ , \tag{38}$$

all in atomic units.

Thus for small displacements we have specified the $a(r)$ and $b(r)$ functions in Eq. (35). A model consisting of the asymptotic predictions for *all* ion pairs *plus* Eq. (35) for the first six nearest neighbors should be sufficient for a practical calculation of the light-scattering spectrum of crystalline LiF. In a crystal the first cation shell is well defined and the thermal distortions of the ions from their lattice sites are small enough for the linear $a(r)$ and $b(r)$ functions to be useful. The electrostatics-only results of Tables V and VI show that the induced polarizability is linear in the displacement up to about 0.5 bohr.

In the melt or in a crystal in which cation diffusion is important, however, the model will need modification as very large polarizability fluctuations will occur as cations in the first shell exchange with others outside it. (We envisage a working definition of the first shell as the six nearest cations.) It is implicit in our expectation that the distorted crystal provides a reasonable model of the melt that such events are not too frequent, but they certainly occur in monovalent melts and it is desirable to find forms for $a(r)$ and $b(r)$ with which fluctuations are quenched.

Some indications of the general shape of the $a(r)$ function are available from calculations of (F^-) in the alkali fluorides[18] and of the polarizability of an atom in a spherical box.[32] At both large positive and negative r the slope (da/dr) is expected to fall to zero. For large r the overlap contribution to $\vec{\vec{\alpha}}$ is expected to fall off rapidly and $\vec{\vec{\alpha}}$ should be predicted accurately by CRYST-type calculations. A cutoff function could be fitted to the variation of the CRYST α (F^-) with lattice parameter for the alkali fluorides.[18] Similarly, calculations on distorted CRYST lattices could be used to fit $b(r)$. An even simpler cutoff procedure would be to replace the total polarizability by α (free F^-) for displacements greater than some large value. If $a(r)$ were linear, with the slope calculated above, it would reach the free ion CHF value at $r\approx2.25$ or $R(\text{Li-F})\approx6$ bohr.

Allowing for these modifications we believe that the results of the present paper provide the necessary parameters for a realistic simulation of the light-scattering spectra of LiF crystals and melt. More important, we have demonstrated by direct calculation the physical mechanisms underlying the fluctuating polarization in ionic materials and which are applicable to a wide range of distortion-induced phenomena.

[1]V. Mazzacurati, G Ruocco, G. Signorelli, E. Cazzanelli, A. Fontana, and G. Mariotto, Phys. Rev. B **26**, 2216 (1982).

[2]G. Mariotto, A. Fontana, E. Cazzanelli, F. Rocca, V. Mazzacurati, and G. Signorelli, Phys. Rev. B **23**, 4382 (1981).

[3]C. Raptis and W. Mitchell, J. Phys. C **16**, 2973 (1983); J. Giergiel, K. R. Subaswamy, and P. W. Eklund, Phys. Rev. B **29**, 3490 (1984).

[4]S. C. An, C. J. Montrose, and T. A. Litovitz, J. Chem. Phys. **64**, 3717 (1976).

[5]P. A. Madden and T. I. Cox, Mol. Phys. **43**, 287 (1981).

[6]P. A. Madden, in *Molecular Liquids,* edited by A. J. Barnes *et al.* (Reidel, Dordrecht, 1984).

[7]L. Frommhold, Adv. Chem. Phys. **46**, 1 (1980).

[8]B. Alder and E. L. Pollock, Annu. Rev. Phys. Chem. **32**, 311 (1982).

[9]P. A. Madden and D. J. Tildesley, Mol. Phys. **49**, 193 (1983).

[10]P. W. Fowler and P. A. Madden, Mol. Phys. **49**, 913 (1983).

[11]M. Parinello and M. P. Tosi, Riv Nuovo Cimento **2**, 1 (1979); J. E. Enderby and G. W. Neilson, Adv. Phys. **29**, 323 (1980).

[12]D. E. Logan. Mol. Phys. **51**, 1395 (1984), and references therein for a discussion of the role of higher multipole moments.

[13]P. Mazur, Adv. Chem. Phys. 1, 309 (1958).

[14]C. J. F. Bottcher and P. Bordewijk, *Theory of Electric Polarization* (Elsevier, New York, 1978), Vols. 1 and 2.

[15]J. R. Tessman, A. H. Kahn, and W. Shockley, Phys. Rev. **92**, 890 (1953).

[16]J. N. Wilson and R. M. Curtis, J. Phys. Chem. **74**, 187 (1970).

[17]G. H. F. Diercksen and A. J. Sadlej, Mol. Phys. **47**, 33 (1982).

[18]P. W. Fowler and P. A. Madden, Phys. Rev. B **29**, 1035 (1984).

[19]P. W. Fowler and P. A. Madden, J. Phys. Chem. (to be published).

[20]P. W. Fowler and N. C. Pyper, J. Phys. C (to be published).

[21]G. D. Mahan, Solid State Ionics **1**, 29 (1980).

[22]R. P. Hurst, Phys. Rev. **114**, 746 (1959).

[23]R. E. Watson, Phys. Rev. **111**, 1108 (1958).

[24]That is, the appropriate polarizability is the gas-phase one (see Ref. 14).

[25]A. J. C. Ladd, T. A. Litovitz, and C. J. Montrose, J. Chem. Phys. **68**, 4031 (1979).

[26]A. D. Buckingham, Adv. Chem. Phys. **12**, 107 (1967).

[27]R. W. G. Wyckoff, *Crystal Structures* (Interscience, New York, 1963), Vol. 1.

[28]P. W. Fowler and P. A. Madden, Phys. Rev. B (to be published).

[29]J. G. Kirkwood, Phys. Z. **33**, 57 (1932).

[30]S. F. Boys and F. Bernardi, Mol. Phys. **19**, 553 (1970).

[31]J. R. Hardy and A. M. Karo, in *Light Scattering Spectra of Solids,* edited by G. B. Wright (Springer, Berlin, 1968), p. 99.

[32]P. W. Fowler, Mol. Phys. (to be published).